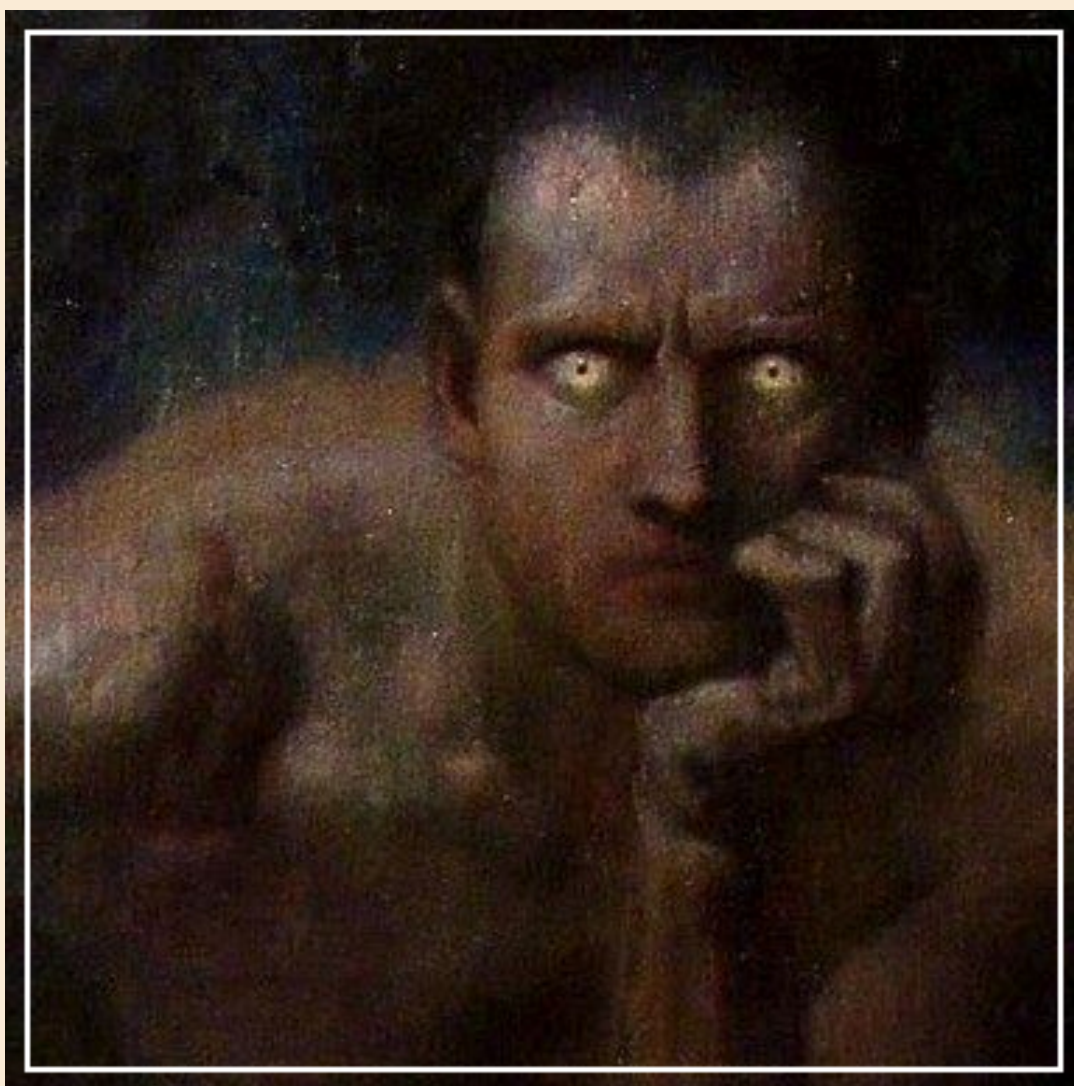


Journal notes on:  
Miscellaneous topics on  
condensed matter physics  
by Francisco Lobo





## CONTENTS

I	Introduction to metals	4
A	Tight-binding band theory	4
1	Bloch's theorem	4
2	Typical examples	4
III	Topological superconductivity	9
A	Josephson junctions	9
1	Andreev bound states	9
2	Majorana zero modes	9
B	Reg-Lutchyn model	9
C	Hartree-Fock-Bogoliubov mean-field theory	9

## I. INTRODUCTION TO METALS

### A. Tight-binding band theory

#### 1. Bloch's theorem

#### 2. Typical examples

##### Linear lattice

*Square lattice* Consider a translation invariant lattice with one atom per unit cell with lattice vectors  $\mathbf{R}_i = a\mathbf{n}_i$  and translation vector vector  $\mathbf{T}$ . The reciprocal square lattice vectors are  $\mathbf{b} = 2\pi/a\mathbf{n}$  corresponding to a squared area 1st Brillouin zone delimited by the vertices  $k = (\pm\pi/a, \pm\pi/a)$ . Suppose that each atom has only one valence orbital  $\phi(\mathbf{r})$ . The corresponding Bloch wavefunction will read as

$$\psi_{\mathbf{k}}(\mathbf{r}) = \frac{1}{\sqrt{N}} \sum_i \exp(i\mathbf{k} \cdot \mathbf{R}_i) \phi(\mathbf{r} - \mathbf{R}_i) \quad (1)$$

See that this is indeed a Bloch function because if  $\mathbf{R}_m$  is a lattice vector so is  $\mathbf{R}_m - \mathbf{T}$ , and thus

$$\begin{aligned} \psi_{\mathbf{k}}(\mathbf{r} + \mathbf{T}) &= \frac{1}{\sqrt{N}} \sum_i \exp(i\mathbf{k} \cdot \mathbf{R}_i) \phi(\mathbf{r} - \mathbf{R}_i + \mathbf{T}) \\ &= \frac{1}{\sqrt{N}} \exp(i\mathbf{k} \cdot \mathbf{T}) \sum_i \exp(i\mathbf{k} \cdot (\mathbf{R}_i - \mathbf{T})) \phi(\mathbf{r} - (\mathbf{R}_i - \mathbf{T})) \\ &= \exp(i\mathbf{k} \cdot \mathbf{T}) \psi_{\mathbf{k}}(\mathbf{r}) \end{aligned} \quad (2)$$

The expectation energy of the Hamiltonian of such a system reads

$$E_{\mathbf{k}} \equiv \langle \mathbf{k} | H | \mathbf{k} \rangle = \frac{1}{N} \sum_{ij} \exp(i\mathbf{k} \cdot (\mathbf{R}_j - \mathbf{R}_i)) \langle \phi_i | H | \phi_j \rangle \quad (3)$$

where  $\phi_i = \phi(\mathbf{r} - \mathbf{R}_i)$ . In a nearest neighbors scheme we define  $\langle \phi_i | H | \phi_i \rangle = -\mu$  as the onsite energy,  $\mu$  being the Fermi level,  $\langle \phi_i | H | \phi_j \rangle = -t$  as the hopping energy between  $i, j$  nearest neighbors apart by a given  $\mathbf{R}_j$  vector and  $\langle \phi_i | H | \phi_j \rangle = 0$  otherwise. In this scheme we write

$$E_{\mathbf{k}} = -\mu - t \sum_{\langle i, j \rangle} \exp(i\mathbf{k} \cdot \mathbf{R}_j) \quad (4)$$

where the sum denoted with the bracket  $\langle i, j \rangle$  is over nearest neighbors only.

In a typical 2D square lattice, the collection of neighboring vectors  $\mathbf{R}_j$  are at  $\{\mathbf{R}_j\} = \{(a, 0), (-a, 0), (0, a), (0, -a)\}$  with  $a$  the lattice constant, so that we obtain

$$E_{\mathbf{k}} = -\mu - 2t (\cos(k_x a) + \cos(k_y a)). \quad (5)$$

See that, as  $\cos$  ranges between  $-1$  and  $1$  the energy  $E_{\mathbf{k}}$  ranges between  $-\mu - 4t$  and  $-\mu + 4t$ , giving a band width of  $8t$ . If one fixes the chemical potential at  $\mu = -4t$  then the conduction band will range

from  $[0, 8t]$ . Near the top and bottom of bands, we will have a quadratic dependence on  $\mathbf{k}$ . Near  $\mathbf{k} = 0$  we can expand the  $\cos$  functions as  $\cos \theta \approx 1 - 1/2\theta^2$ , obtaining a free-electron-like energy structure,

$$\begin{aligned} E_{\mathbf{k}} &\approx -\mu - 2t \left( 1 - \frac{1}{2}k_x^2 a^2 + 1 - \frac{1}{2}k_y^2 a^2 \right) \\ &= -\mu - 4t + t(k_x^2 + k_y^2) a^2, \end{aligned} \quad (6)$$

of circular constant-energy surfaces near the center of the Brillouin zone. Similarly, if both  $k_x$  and  $k_y$  are close to Brillouin zone edge, i.e  $k_i = \pi/a - \delta_i$  with  $i = x, y$ , we obtain

$$\begin{aligned} E_{\mathbf{k}} &= -\mu - 2t (\cos(\pi - \delta_x a) + \cos(\pi - \delta_y a)) \\ &= -\mu - 2t (\cos(\pi) \cos(\delta_x a) - \sin(\pi) \sin(\delta_x a) + \cos(\pi) \cos(\delta_y a) - \sin(\pi) \sin(\delta_y a)) \\ &= -\mu + 2t (\cos(\delta_x a) + \cos(\delta_y a)) \\ &= -\mu + 4t - t(\delta_x^2 + \delta_y^2) a^2 \end{aligned} \quad (7)$$

which also gives circular constant-energy surfaces near the zone corners. On the other hand, see that, for example, the solution to which  $\cos(k_x a) + \cos(k_y a) = 0$  holds true is  $k_x a = \pi - k_y a$ , being straight lines.

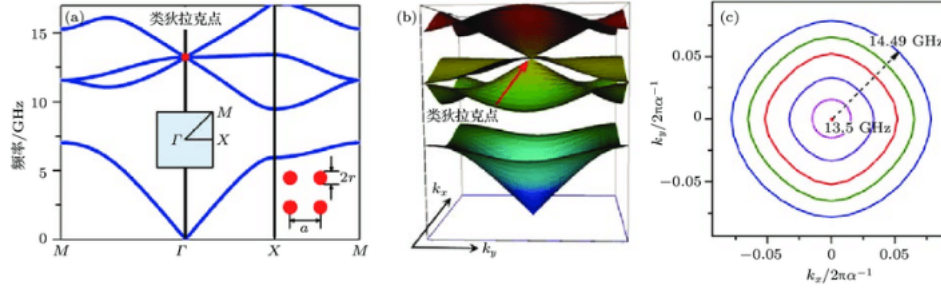


Figure 1. Will eventually fix the image. This is stole and not exactly just simply square.

In a similar tight-binding approach, we could start by instead expressing the Hamiltonian in terms of creation and annihilation fermion operation,  $c^\dagger$  and  $c$ , and the momentum operator  $\mathbf{p} = -i\nabla$ , with  $\nabla = (\partial_x, \partial_y)$  the gradient operator, as

$$H(\mathbf{r}) = c^\dagger(\mathbf{r}) (-\eta \nabla^2 - \mu) c(\mathbf{r}), \quad (8)$$

with  $\eta$  a constant dependent on the effective mass of the electrons.

Discretizing the  $x$  and  $y$  directions by the lattice constant  $a_0$ , corresponding to the  $i, j$  sites positions, the partial derivatives (in central differencing) follow as, for example in the  $x$  direction,

$$\nabla c(\mathbf{r}) \rightarrow \frac{1}{2a_0} (c_{(i+1)} - c_{(i-1)}) = \frac{1}{2a_0} \begin{pmatrix} 0 & 1 & 0 \\ -1 & 0 & 1 \\ 0 & -1 & 0 \end{pmatrix} \begin{pmatrix} c_{(i-1)} \\ c_i \\ c_{(i+1)} \end{pmatrix} \quad (9)$$

and consequently

$$\nabla^2 c(\mathbf{r}) \rightarrow \frac{1}{a_0^2} (c_{(i+1)} - 2c_i + c_{(i-1)}) = \frac{1}{a_0^2} \begin{pmatrix} -2 & 1 & 0 \\ 1 & -2 & 1 \\ 0 & 1 & -2 \end{pmatrix} \begin{pmatrix} c_{(i-1)} \\ c_i \\ c_{(i+1)} \end{pmatrix} \quad (10)$$

Hence, in this discretized space, we have that

$$c^\dagger(\mathbf{r}) (-\eta \nabla^2 - \mu) c(\mathbf{r}) \rightarrow \begin{pmatrix} c_{i-1}^\dagger & c_i^\dagger & c_{i+1}^\dagger \end{pmatrix} \begin{pmatrix} 2t - \mu & -t & 0 \\ -t & 2t - \mu & -t \\ 0 & -t & 2t - \mu \end{pmatrix} \begin{pmatrix} c_{i-1} \\ c_i \\ c_{i+1} \end{pmatrix}$$

Performing the matrices multiplication we obtain

$$\left( c_{i-1}^\dagger (2t - \mu) c_{i-1} - c_{i-1}^\dagger t c_i \right) + \left( -c_i^\dagger t c_{i-1} + c_i^\dagger (2t - \mu) c_i - c_i^\dagger t c_{i+1} \right) + \left( -c_{i+1}^\dagger t c_i + c_{i+1}^\dagger (2t - \mu) c_{i+1} \right)$$

which can be compactly written as

$$H_K = (2t - \mu) \sum_i c_i^\dagger c_i - t \sum_{\langle i,j \rangle} c_i^\dagger c_j \quad (11)$$

The complete energy spectrum can then be obtained numerically by solving for the eigenvalues of the Hamiltonian. Moreover, one could also solve numerically for the density matrix of the system to check upon the local density of energy of states of said energies. This is will be explored further again in Part II on Section ??.

#### *Example: Honeycomb lattice (hBN)*

Hexagonal boron nitride (hBN) is a 2D material composed of a simple layer of alternating boron and nitrogen atoms disposed in a planar honeycomb lattice, as shown in Fig.(2)(a). hBN shares a lot of similarities with graphene, also a 2D honeycomb structured material but instead composed of only carbon atoms. The most relevant distinction is that graphene behaves as a semi-metal with a zero-gap at its Dirac points while hBN, due the different electrostatic environment in the boron and in the nitrogen atom, has an opening gap of about  $\epsilon_g = 5.9\text{eV}$  (there are actually a lot of different results for  $\epsilon_g$  in the literature however the mentioned value is one of the more commonly reported [Ca16]). Also, hBN has a slightly larger lattice constant than graphene (about 1.8%), being around  $a_0 = 2.5\text{\AA}$  [Ish03]. The planar honeycomb lattice can be described as a triangular Bravais lattice generated by the real vectors basis  $\mathbf{a}_1 = a_0/2 (1, \sqrt{3})$  and  $\mathbf{a}_2 = a_0/2 (-1, \sqrt{3})$ . In each Wigner-Seitz cell, we have one atom of boron and one atom of nitride, which we designate as sub-lattices  $A$  and  $B$  respectively, having positions,  $\mathbf{s}_A = (0, 0)$  and  $\mathbf{s}_B = a_0/\sqrt{3}(0, 1)$ . For each site  $A$ , the position of the nearest-neighbors (NN) in the sites  $B$  are given by  $\boldsymbol{\delta}_1 = a_0/\sqrt{3}(0, 1)$ ,  $\boldsymbol{\delta}_2 = a_0/(2\sqrt{3})(-\sqrt{3}, -1)$  and  $\boldsymbol{\delta}_3 = a_0/(2\sqrt{3})(\sqrt{3}, -1)$ . All these vectors are shown in Fig.(2)(a) within the real space lattice. Furthermore, from the real lattice basis vectors follow the reciprocal lattice basis vectors  $\mathbf{b}_1 = 2\pi/(\sqrt{3}a_0)(\sqrt{3}, 1)$  and  $\mathbf{b}_2 = 2\pi/(\sqrt{3}a_0)(-\sqrt{3}, 1)$ , which are shown in Fig.(2)(b) together with the first zone of Brillouin, which they form.

In order to compute the excitonic energies using Eqs.(?) through (?), we first need to know the single-particle Bloch wave-functions  $\phi_{\mathbf{k}\lambda}$ . In this work we calculate them in a nearest-neighbors tight-binding model. For this, we write the system's single-particle NN tight-binding Hamiltonian in real space as

$$H_{\text{TB}}(\mathbf{R}) = \sum_i \epsilon_A a_{\mathbf{R}_i}^\dagger a_{\mathbf{R}_i} + \sum_i \epsilon_B b_{\mathbf{R}_i}^\dagger b_{\mathbf{R}_i} - t \sum_{\langle i,j \rangle} \left( a_{\mathbf{R}_i}^\dagger b_{\mathbf{R}_i + \boldsymbol{\delta}_j} + b_{\mathbf{R}_j}^\dagger a_{\mathbf{R}_i - \boldsymbol{\delta}_j} \right), \quad (12)$$

where the operators  $a_{\mathbf{R}_i}^\dagger (a_{\mathbf{R}_i})$  create (annihilate) an electron in the sub-lattice  $A$  in a given Bravais lattice site  $\mathbf{R}_i$  while the operators  $b_{\mathbf{R}_i}^\dagger (b_{\mathbf{R}_i})$  create (annihilate) an electron instead in the sub-lattice  $B$  (in a given Bravais lattice site  $\mathbf{R}_i$ ). Therefore, the first two terms correspond to the isolated

single-particles Hamiltonian of the site  $A$  and  $B$ , respectively, and the last term to the hybridization between neighboring sites  $i$  and  $j$ , describing the possible hoppings from site  $A$  to site  $B$  and vice-versa. We only assess hopping terms up to the first neighbors terms, which is denote by  $\langle i, j \rangle$ , and consider a static hopping term in either direction, i.e  $t_{\mathbf{R}_i, \mathbf{R}_j} \rightarrow -t$ . Notice that, contrarily to graphene, since the atoms on sites  $A$  and  $B$  are different the single-particle energies  $\epsilon_A$  and  $\epsilon_B$  are inherently different. We can represent the NN TB Hamiltonian in Eq.(12) in reciprocal space by expressing the creation/annihilation operators as their Fourier counterparts,

$$a_{\mathbf{R}_i} = \frac{1}{\sqrt{V}} \sum_{\mathbf{k}} e^{+i\mathbf{k} \cdot (\mathbf{R}_i + \mathbf{s}_A)} a_{\mathbf{k}} \quad \text{and} \quad b_{\mathbf{R}_i} = \frac{1}{\sqrt{V}} \sum_{\mathbf{k}} e^{+i\mathbf{k} \cdot (\mathbf{R}_i + \mathbf{s}_B)} b_{\mathbf{k}} \quad (13)$$

and rearranging the expression just that the identity  $\delta(\mathbf{k} - \mathbf{k}') = 1/N \sum_i e^{-i\mathbf{R}_i \cdot (\mathbf{k} - \mathbf{k}')}$  is apparent. We obtain

$$H_{\text{TB}}(\mathbf{R}) = \sum_{\mathbf{k}} \epsilon_A a_{\mathbf{k}}^\dagger a_{\mathbf{k}} + \sum_{\mathbf{k}} \epsilon_B b_{\mathbf{k}}^\dagger b_{\mathbf{k}} - t \sum_{\mathbf{k}} \left( \gamma_{\mathbf{k}} a_{\mathbf{k}}^\dagger b_{\mathbf{k}} + \gamma_{\mathbf{k}}^\dagger b_{\mathbf{k}}^\dagger a_{\mathbf{k}} \right), \quad (14)$$

with the newly-defined  $\gamma$  complex number  $\gamma_{\mathbf{k}} = \sum_{\langle j \rangle} \exp(+i\mathbf{k} \cdot \boldsymbol{\delta}_j)$ . If we now define a row vector  $c_{\mathbf{k}}^\dagger = [a_{\mathbf{k}}^\dagger \ b_{\mathbf{k}}^\dagger]$  we can rewrite the system's Hamiltonian as  $H_{\mathbf{R}}^{\text{TB}} = \sum_{\mathbf{k}} c_{\mathbf{k}}^\dagger H_{\mathbf{k}}^{\text{TB}} c_{\mathbf{k}}$  with the hBN NN TB Hamiltonian matrix being

$$H_{\text{TB}}(\mathbf{k}) = \begin{bmatrix} \epsilon_A & -t\gamma_{\mathbf{k}} \\ -t\gamma_{\mathbf{k}}^\dagger & \epsilon_B \end{bmatrix}. \quad (15)$$

Within this simplified tight-binding model, the expression for the electronic two-band structure can easily be obtained analytically by diagonalizing the matrix in Eq.(15), yielding

$$E_{\text{TB}}^\pm(\mathbf{k}) = \pm \sqrt{\epsilon^2 + t^2 \left[ 3 + 2 \cos(a_0 k_x) + 4 \cos\left(\frac{a_0 \sqrt{3}}{2} k_y\right) \cos\left(\frac{a_0}{2} k_x\right) \right]}. \quad (16)$$

Here we defined the zero point energy at  $(\epsilon_A + \epsilon_B)/2$  and defined  $\epsilon \equiv (\epsilon_A - \epsilon_B)/2$  at the middle of the gap such that  $\epsilon_A = \epsilon$  and  $\epsilon_B = -\epsilon$ . The valence band corresponds to the  $E_{\text{TB}}^-(\mathbf{k})$  dispersion while the  $E_{\text{TB}}^+(\mathbf{k})$  corresponds to the conduction band, as shown in Fig.(2)(c) which is accompanied by the density of states  $\text{DoS}(E) = \sum_{\mathbf{k}} \delta(E - E(\mathbf{k}))$ . Notice that, if  $\epsilon_A = \epsilon_B$ , as is the case for graphene, we obtain  $\epsilon = 0$  and the band dispersion closes in a linear fashion at the so called Dirac points,  $\mathbf{K}^\pm = (\pm 4\pi/(3a_0), 0)$ . In hBN, the electronic band dispersion is also at its minimum near these points but has instead a parabolic shape. In either case, this points represent a fundamental symmetry of the system, called valley parity. To see why the dispersion is parabolic at these valley points, we Taylor series expand the exponential of  $\gamma_{\mathbf{k}}$  in Eq.(??) near  $\mathbf{k} \rightarrow \mathbf{K} + \mathbf{p}$  with  $\mathbf{p} \rightarrow 0$ . We obtain  $\exp(+i\mathbf{p} \cdot \boldsymbol{\delta}_j) \approx 1 + i\mathbf{p} \cdot \boldsymbol{\delta}_j$ . Now, since  $\sum_{\langle j \rangle} \exp(+i\mathbf{K} \cdot \boldsymbol{\delta}_j) = 0$  we are left with  $\gamma_{\mathbf{K}+\mathbf{p}} \simeq i\mathbf{p} \cdot \sum_{\langle j \rangle} \exp(+i\mathbf{K} \cdot \boldsymbol{\delta}_j) \boldsymbol{\delta}_j = -\sqrt{3}a_0/2 (p_x - ip_y)$ . Invoking the Pauli matrices definitions, from Eq.(15) we can write the TB Hamiltonian  $H_{\text{TB}}^{\mathbf{k}}$  in this low-energy regime as

$$H_{\text{TB}}(\mathbf{K} + \mathbf{p}) = \epsilon \sigma_z + t \frac{\sqrt{3}a_0}{2} (\mathbf{p} \cdot \boldsymbol{\sigma}), \quad (17)$$

which clearly resembles the 2D Dirac Hamiltonian,  $H_{\text{Dirac}} = \sigma_z mc^2 + c(\mathbf{p} \cdot \boldsymbol{\sigma})$  with  $\epsilon$  taking the role of the rest mass energy  $mc^2$  and instead with a velocity  $v_F = t\sqrt{3}a_0/2$ , termed the *Fermi velocity*, as a replacement to the velocity of light  $c$ . Notice that, for the case of graphene, since  $\epsilon = 0$ , the electrons

would behave as if they are massless. In this limit, the hBN low-energy dispersion can be written as the typical relativistic dispersion relation

$$E_{\text{TB}}(\mathbf{K} + \mathbf{p}) = \pm \sqrt{p^2 v_F^2 + m_{\text{eff}}^2 v_F^4}. \quad (18)$$

where  $m_{\text{eff}}$  is the effective mass of the electron at a given point near the valleys.

Although not captured in this simple tight-binding model, if one does some type of DFT to obtain a more complete electronic band structure, one could see that the hBN bands do actually cross between themselves (see, for example, Fig.(1) from [Fe19]). This appears to be troublesome to our two-band time-dependent Hartree-Fock mean-field theory since certain transitions could occur between bands that are not accounted for in our model. However, these other intersecting bands corresponds to electronic states that are orthogonal to the ones we use in our two-band model and thus, will not interfere (i.e, even if we accounted for this other bands in our model, the form factors in Eqs.(??)-(??) would always give zero for transitions between those bands). However, this only applies for the hBN case since, if one was dealing instead with TMDs, one would need to account for at least three bands [Li13]. Furthermore, following the context of TMDs, one should also need to account for the spin-orbit coupling (SOC) where the effective Hamiltonian for such a system could be obtained by adding to Eq.(17) the term  $H_{\text{SOC}} = t_s t_z (\sigma_z - 1)/2$  where  $t_s$  quantifies the spin-orbit coupling and  $s_z = \pm 1$  labels the spin projection of the bands [Li13, Sch17].

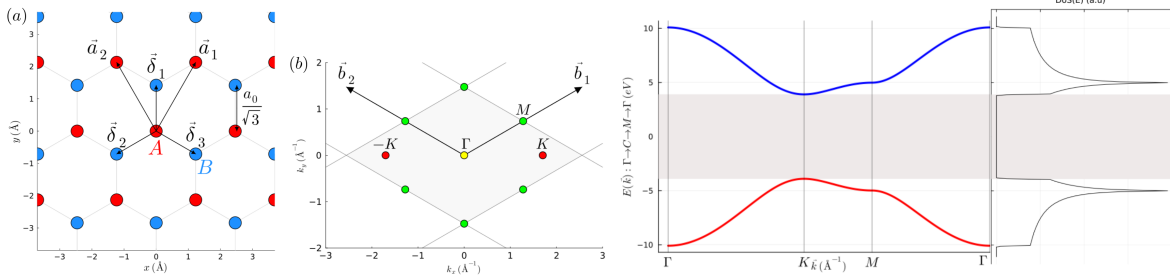


Figure 2. (a) hBN real space honeycomb lattice constructed from two superposed triangular sub-lattices of boron atoms (depicted in red), denoted as sub-lattice A, and of nitrogen atoms (depicted in blue), denoted as sub-lattice B. The vectors  $\mathbf{a}_1$  and  $\mathbf{a}_2$  are the lattice basis vectors and  $\delta_1$ ,  $\delta_2$  and  $\delta_3$  are the nearest-neighbor vectors. (b) hBN reciprocal space lattice with  $\mathbf{b}_1$  and  $\mathbf{b}_2$  its basis vectors. The first Brillouin zone is emphasized in light gray while the remaining are only outlined. The red dots correspond to the Dirac points  $\pm K$  and the green dots correspond to the 1BZ edges  $M$  points. (c) hBN electronic band structure from a nearest-neighbor tight-binding model accompanied by the density of the states. The dispersion goes along the symmetry path  $\mathbf{k} : \Gamma \rightarrow K \rightarrow M \rightarrow \Gamma$  and was calculated using  $\epsilon_g = 7.8\text{eV}$  for the energy gap,  $t = 3.1\text{eV}$  for the hopping parameter and  $a_0 = 1.42\sqrt{3}\text{\AA}$  for the honeycomb lattice length.



## II. TOPOLOGICAL SUPERCONDUCTIVITY

### A. Josephson junctions

1. *Andreev bound states*

2. *Majorana zero modes*

### B. Oreg-Lutchyn model

### C. Hartree-Fock-Bogoliubov mean-field theory

Here goes the appendix of the 1st paper